Fermi National Accelerator Laboratory

Study of Azimuthal quench propagation in 11 T dipole magnet

Samuele Mariotto

Supervisor: Prof. Emanuela Barzi
Co-Supervisor: Prof. Alexander Zlobin

Final Report
Summer School Internship

.

25 July - 23 September 2016

Contents

Introduction

The 11 T Dipole Magnet

The Large Hadron Collider (LHC) works from 2010 with proton beam packed in *bunches* at 3.5 TeV each for a total of 7 TeV in the mass center's frame of the colliding bunches. From the $2013-2014$ Shutdown the energy of the bunches has been upgraded at 7 TeV for a total of 14 TeV in the mass center frame. Many USA research centers contribute to the planned upgrades of the Large Hadron Collider in the LARP collaboration. To satisfy these required upgrades CERN and FNAL achieved a joint R&D program to develop an 11 T dipole magnet compatible with LHC main lattice providing space for additional collimators in the dispersion suppressor (DS) areas around CMS and ATLAS detectors. The 8.33 T 15 m long Nb-Ti main dipoles will be substitued with shorter 11 T Nb_3Sn dipoles delivering the same 119 Tm strength at the operational current of 11.85 kA of LHC strands and leaving other space for the additional collimators. As a first stage a 2 m long single-aperture Nb_3Sn dipole demonstrator MBHSP01 was developed, fabricated and tested at FNAL in June 2012. After the tests made at the FNAL laboratories to study the magnet design and fabrication process, the quench performance and field quality, two other 1 m prototypes MBHSP02 and MBHSP03 were developed and tested in single-aperture configuration and then in a common iron yoke.

This report and the work presented here concern about the quench protection of superconducting magnets for high energy particle accelerators and in particular for the 11 T dipole magnet developed for the LHC upgrade. The quench is the transition of the superconductive material to the resistive or normal conductive state due, tipically, to an amount of energy released in the material that

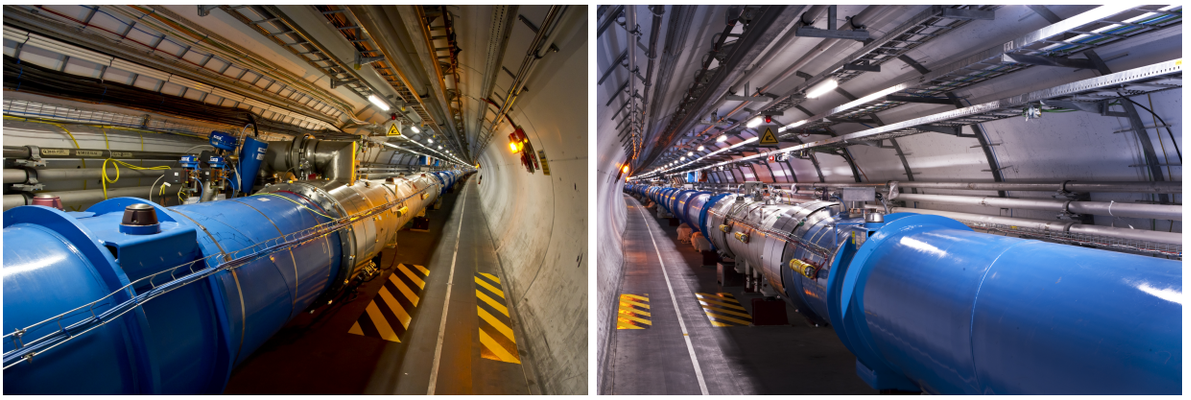

Figure 1: Large Hadron Collider.

causes an increase of the temperature over its critical limit. The quench protection of the present-day high field Nb_3Sn accelerator magnets is based on resistive protection heaters, typically stainless steel laminates on the coil surfaces. They bring large segments of the winding to a resistive state during the quench, accelerating the magnet current decay and consequently reducing the hotspot temperature preventing the damage of the magnet or the melt of the materia itself. In this work there is presented the study of the heat propagation (created by the quench heaters) through the superconductive material of the accelerator and the isolation layers that cover the superconducting material itself. Quench heaters strip are connected directly to the magnet coils and are in thermal contact with the insulation layers and the superconducting material. This work focuses on the study of the quench delay time as function of the single turns considered in the magnet's coils and the quench difference delay time as a function of the operational current of the magnet itself.

Quench delay time: is the time measured from the activation point of the quench heaters to the detection of the quench in the single turn of the magnet's coil.

Quench delay time difference: Difference of quench delay time measured between HF turns (High Field strenght) and LF turns (Low Field strength) of the same coil.

We aim to the solution of discrepancy between measurements and simulations of these parameters made up both at FNAL laboratories and at Cern. All these measurements and Simulation were made on the prototypes of 11 T dipole magnet.

We show the results of the simulation made up to better understand the dependance of the quench delay time and the quench difference delay time from several parameters. At the end we compare the results of the simulations to the FNAL data and Cern data showing the goals we obtained and the possible develops of our study on the Quench protection system through the use of the quench heaters.

Chapter 1

Quench Delay Time Difference

1.1 Start of the quench

We are firstly interested in the determination of the start of quench in the superconducting material. This parameter depends on the operation point of the magnet. The superconducting material shows a normal conductive or resistive state when the operation point is over the so called "Critical Surface". The main parameters to determine this particular surface are the temperature, the magnetic field strength and the current density that flows in the superconducting material. In our case, the value of the current density is fixed by the value of the total current that is necessary to create an 11 T magnetic field strength (11850 A) and by the cross section of the cable itself.

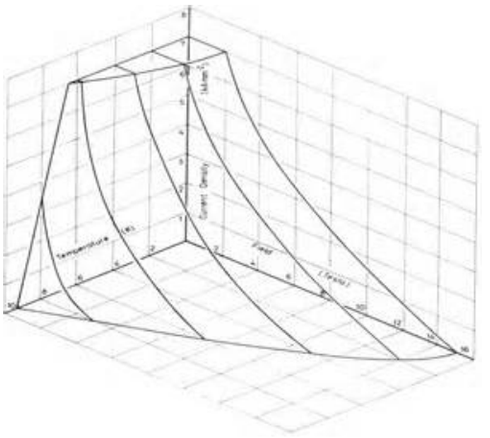

Figure 1.1: Critical Surface of a supercnducting material as function of the Magnetic Field Strength, Current and Temperature

If only one of the others parameters is above the equivalent critical value, the superconducting state turns in the normal resistive state and the quench starts in the cable of the magnet. To better undestand the development of the quench we would need to consider the balance between the heat exchange and the adiabatic heat generation in the superconducting material. If the amount of heat exchanged by the quenched material is more than the amount of heat absorbed by the material, the quenched volume will decrease and the superconducting state is restored. On the other hand if the amount of heat exchanged is less than the value of heat generated, the quench will

propagate in the material, thus increasing the speed of the transition of the superconducting cable. Studying the material property at different temperatures, we could estimate the size of the minimum propagating zone (MPZ) that determines the minimum value of volume that has to be heated in order to create a never ending transition of the material itself. In our model we will not consider the calculation of the minimum propagating zone because of the difficulty of implementation of this way of quench detection in a c++ code. However, other more complicated and developed models (like Qlasa, developed at the Lasa laboratories in Milan, or Roxie, developed at Cern) take into account this particular way of quench detection in order to have more precision in the quench delay time determination. In our model we are interested in the difference of the operational point between the High field turns (HF) and Low field turns (LF) in the outer layer of the dipole. At the operational value of current (11850 A), the average values of magnetic field intensity in the firt turns of this two sections of the magnet are 10T and 5.3T. This difference can be also considered in the equivalent temperature margin from the value of the critical temperature of the superconducting material. Studying the maps reported in figure 1.2, taken by simulation using Roxie

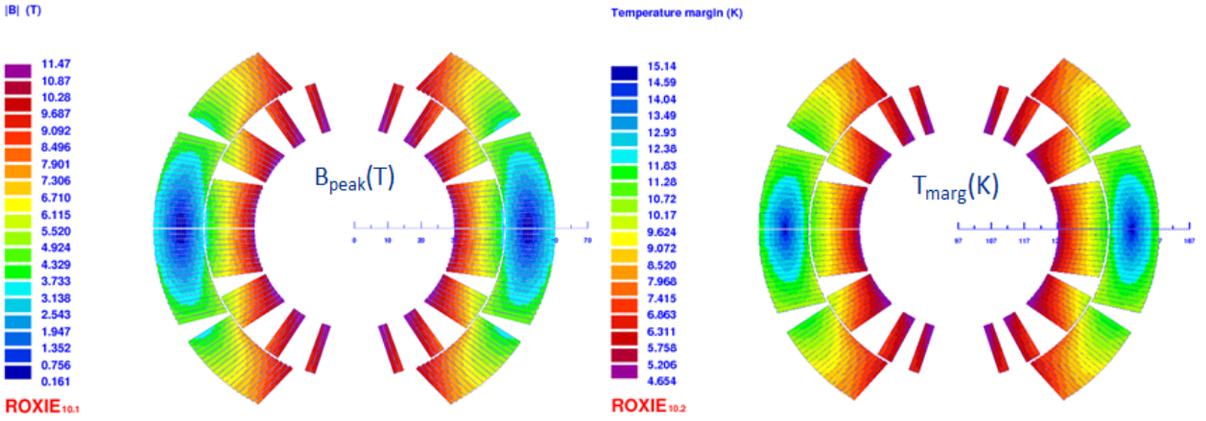

Figure 1.2: Magnetic Field and Temperature Margin distribution in the superconducting turns of the MBHSP02 prototype, ROXIE, Cern

we could observe that a higher value of magnetic field strength corresponds to a lower temperature margin. We expect the quench delay time of HF turns to be smaller compared with the LF turns' once. In fact, in figure 1.3 we can see that the point A (HF turns), at fixed a given time after the heaters start, develops a higher temperature than the point B (LF turns), thus showing the quench before the LF Turns.

However we are not interested only in the quench delay time but also in the calculation of the quench delay time difference. In particular, we would like to study its dependance from the current that flows in the superconducting cable. In principle, focusing only on the two types of turns, we can establish the behaviour of the quench delay time difference. If the current is almost 0 the difference of the magnetic field intensity in which the superconducting turns are operating is very small. The operating points of the two types of the turns are very close and this leads to close values of the quench delay time giving a null quench delay time difference. Increasing the current, the difference between the magnetic field strength is higher giving as a result an increasing value of the quench delay time difference. This expected behaviour can be seen in the simulations made on prototypes for the 11T dipole magnet developed both at Cern and Fermilab.

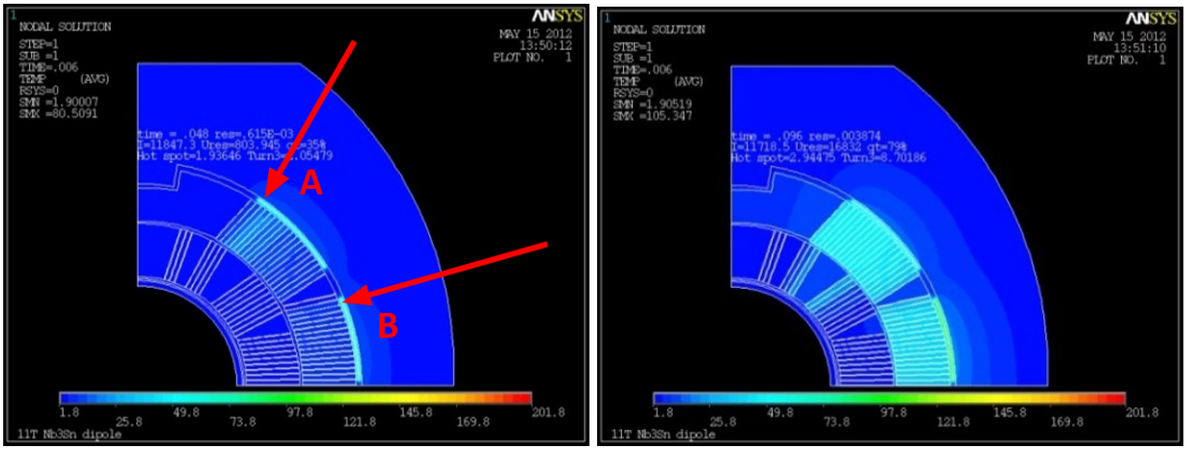

Figure 1.3: Simulations of the propagation of heat at different time made with ANSYS

1.2 Problem: Discrepancy between experimental Data and Simulations

The main problem that I tried to solve is the difference between the experimental data of the quench delay time difference and the simulation data that try to describe the reliance of this parameter on the current which flows into the superconducting cable. In the following pictures we can see the two different and completely independent measurements and simulations made by Cern and Fermilab on two prototypes of the 11 T dipole magnet [1].

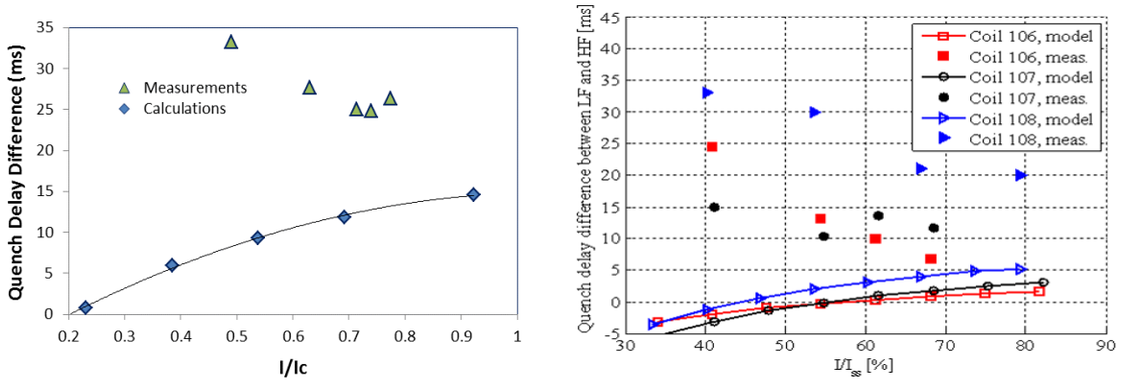

Figure 1.4: Quench delay time difference: comparison between measurements and simulations. FNAL prototype (left plot), CERN prototype (right plot).

Measurements do not have the same behaviour of the simulation as we could expect. With very low values of the current they seem to diverge while for high values of the current they decrease. Instead, simulations start with values of the quench difference delay time close to 0 at small values of the current and increase with higher values of this last parameter. Moreover, simulations seem to saturate at high value of current. It is interesting to observe that different and indipendent experimental measurements have the same behaviour, and this particular behaviur is completely

different from that of the simulations carried out giving the hint of a non well comprehension of the propagation of the heat in the superconducting material.

To solve the discrepancy between the experimental data and the measurements, we inserted, in the propagation of the heat from the quench heaters to the superconducting cable, a so called additional ¨*Contact resistance*¨.

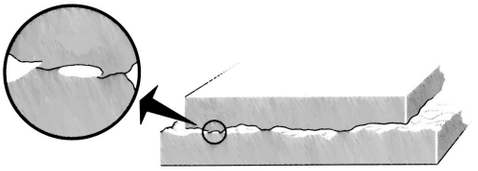

This additional parameter is principally due to the non ideal thermal connection of the materials at their surfaces among the quench heaters and the superconducting cable. In the heat transfer between the heaters and the superconducting cable there are three different interfaces:

- From the stainless steel (quench heaters) to Kapton
- From Kapton to G10
- From G10 to the Cable

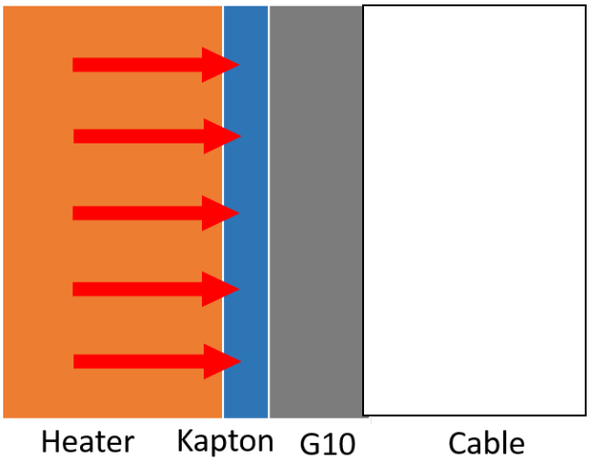

Figure 1.5: Interfaces of the different materials

As a consequence, there can be, in principle, three different contact resistances, one for each interfaces, but we used only one of them for semplicity. We considered only the interface between the G10 and the Cable but, for further development, we could extend the number of the contact resistances. This additional parameter is not only a simple constant (if so, it would not affect the quench delay time difference, but only the single quench delay time of each turn in the same way). To have a different value of the quench delay time difference as function of the current, we need that the contact resistance also to be a function of the operational current. We supposed the

contact resistance to be a function of the pressure inside the magnet between each layer of different materials.

$$k(T) = \frac{1}{\lambda(T)\Delta L + R_{th}^{contact}(P)} \tag{1.1}$$

We considered the dependance from the pressure because it determines the equivalent amount of surface that is really in thermal contact at the material surface through which the heat can flow reaching the superconducting cable. Considering the equivalent total resistance as the sum of two independent resistance (contact and thermal), we obtain:

$$k(T) = \frac{1}{\lambda(T)\Delta L + \frac{1}{\alpha P + \beta}} \tag{1.2}$$

We supposed an inversion proportion to the pressure for the contact resistance but this is only the first approximation. We could, in principle, increase the order of the polynomial dependance from the pressure selecting for each of the power a free parameter that has to be calculated or extracted by fitting with experimental data. We introduced only two parameters α and β considering the first order of the dependance from pressure. However, unfortunately, we do not have detailed values of the pressure inside the magnet so we have to rewrite this parameter as function of others known physical dimensions. The pressure can be written as a function of the local magnetic field strength and the current that flows in the superconducting cable because the radial force that determines the surface really in thermal contact is the Lorentz force acting on a filament crossed by current and operating in a fixed value of external magnetic field strength. In addition, the magnetic field can be written as a local function of the current itself and the position in which we are calculating the pressure.

$$k(T) = \frac{1}{\lambda(T)\Delta L + \frac{1}{\alpha'' \gamma I^2 + \beta}} \tag{1.3}$$

We could so rewrite the contact resistance as a function of the operating current, selecting only the two parameters alpha and beta and calculating the dependance of the magnetic field by the position. For this last point we used in our model the magnetic field strength as function of the position considering it an input data. We used the field map created with Roxie (developed at Cern) to calculate the value of the field in the first HF turn and in the first LF turn (see figure 1.2).

The contact resistance is so only an explicit function of the magnetic field current with two degree of freedom that we can adjust with the two parameters to fit the experimental data in order to get the value of the contact resistance itself.

Chapter 2

Finite Element Model

2.1 Heat Transfer Equation

We have to determine the time in which the superconductive material shows the transition to the conductive and resistive state. To reach this goal I developed a c++ code to solve the equation of the heat transfer [3][2]. The heat is generated from the quench heaters and it flows through the isolation layers reaching the supercoductive material. Its flow depends upon the material properties like the Therma Conductivity and the Specific Heat of the layers between the heaters and the superconducting cable. We decided to study the heat transfer only in one dimension for the simmetry of the elements in the magnet. In fact, if we consider the stainless steel strips, the heat is generated in all its width and so, for different turns, it is uniform. We could not consider the heat transfer from adiacent turns (Second Dimension) because at the same time they are at an equal value of temperature. The third dimension is the lenght of the magnet: beacuse of the magnet is uniform for all its length in the beam axis direction that is over 5 meter and because of, in the cross section plane, we are considering dimensions of mm of lenght, we could focuse only in the radial direction (cross section plane). This is the equation we need to solve:

$$\frac{\partial}{\partial x}\left[k(T)\frac{\partial T}{\partial x}\right] + \frac{\rho(T)I^2}{A^2} = c_p^c(T)\delta(T)\frac{\partial T}{\partial t} \tag{2.1}$$

In the 11 T dipole magnet the heat is totally generated in the quench heaters but it could be generated also in the cable if the material is in the conductive resistive state. However, in the First Model we developed, we made two approximations:

- The heat is at first entirely generated in the heaters and, after the time necessary to generate the transition, it flows through the isolation layers reaching the superconducting cable.
- The aim of the simulation is to determine the quench delay time i.e. the time in which the material of the cable shows the transition. Thus the simulation ends while, at the same time, the heat is generated in the cable.

We can therefore simplify the equation that we are trying to solve negletting the in time generation leading to the following equation:

$$\frac{\partial}{\partial x}\left[k(T)\frac{\partial T}{\partial x}\right] = c_p^c(T)\delta(T)\frac{\partial T}{\partial t} \tag{2.2}$$

It is useful, however, to modify the equation using adimensional coefficients relating only to adimensional parameters in order to implement a finite element code in which each parameters is a variable of the program itself. A simple way to make all the parameters adimensional is to relate them to their value at the 0 time of the simulation that corresponds in the heat transfer equation to the initial temperature.

We obtained the following equation:

$$\tilde{k}(\theta)\frac{\partial^2\theta}{\partial x'^2} + \frac{\partial\tilde{k}(\theta)}{\partial\theta}\left(\frac{\partial\theta}{\partial x'}\right)^2 = \tilde{c}_p^c(\theta)\tilde{\delta}(T)\frac{\partial\theta}{\partial t} \tag{2.3}$$

Where:

$$\tilde{k}(\theta) = \frac{k(T)}{k(T_0)} \qquad \tilde{\delta}(\theta) = \frac{\delta(T)}{\delta(T_0)}$$

$$\tilde{c}_p^c(\theta) = \frac{c_p^c(T)}{c_p^c(T_0)} \qquad \theta(x', t') = \frac{T(x,t)}{T_0}$$

$$t' = \frac{t}{\frac{c_p^c(T_0)\delta(T_0)L^2}{k(T_0)}} \qquad x' = \frac{x}{L}$$

We substituted all the material properties and also the Temperature, the time and the space with adimensional parameters. This technique is very useful in the determination of the space and time. In fact we can rewrite both these physical dimensions with finite time and space interval and a iterational counter for the implementation in the c++ code.

$$x' = ih, \qquad i = 0, 1...N; \qquad t' = jz, j = 0, 1, 2...; \qquad r = \frac{z}{h^2}$$

Using an iteration code we have to simplify all the derivatives considering each position and time labeled by the counters i and j respectively.

$$\frac{\partial\theta}{\partial t}\Big|_{i,j} \approx \frac{\theta_{i,j+1} - \theta_{i,j}}{z} \qquad \frac{\partial\theta}{\partial x'}\Big|_{i,j} \approx \frac{\theta_{i+1,j} - \theta_{i,j}}{2h}$$

$$\frac{\partial^2\theta}{\partial x'^2}\Big|_{i,j} \approx \frac{\theta_{i+1,j} - 2\theta_{i,j} + \theta_{i-1,j}}{h^2} \qquad \frac{\partial\theta}{\partial x'}\Big|_{0,j} \approx \frac{\theta_{1,j} - \theta_{0,j}}{h}$$

After these simplifications we can obtain:

$$\theta_{i,j+1} = \theta_{i,j} + \frac{r}{(\tilde{c}_p^c)_{i,j}\tilde{\delta}_{i,j}}\left[\tilde{k}_{i,j}(\theta_{i,j+1} - 2\theta_{i,j} + \theta_{i-1,j}) + \frac{1}{4}\left(\frac{\partial\tilde{k}}{\partial\theta}\right)_{i,j}(\theta_{i+1,j} - \theta_{i-1,j})^2\right]$$

To solve the equation we have to set the boundary conditions for the temperature of the material. We can set the initial point of operation: in the original model we set the initial temperature of the heaters equal to 300 K considering this temperature as the fixed valued to refer all the other temperature of the insulation layers and the cable that is 1.9 K:

$$\theta_{0,0} = 1 \quad \theta_{i,0} = \frac{1.9}{300} \tag{2.4}$$

In the upgraded model we set all the material at a uniform temperature simulating, for the heater, the generation of the heat while it flows in the rest of the insulation layer and the cable. We used only:

$$\theta_{i,0} = 1 \tag{2.5}$$

The simulation starts dividing all the material in finite elements of fixed thick and considering the heat exchange of the first elements. At each temporal step, the code calculate the temperature

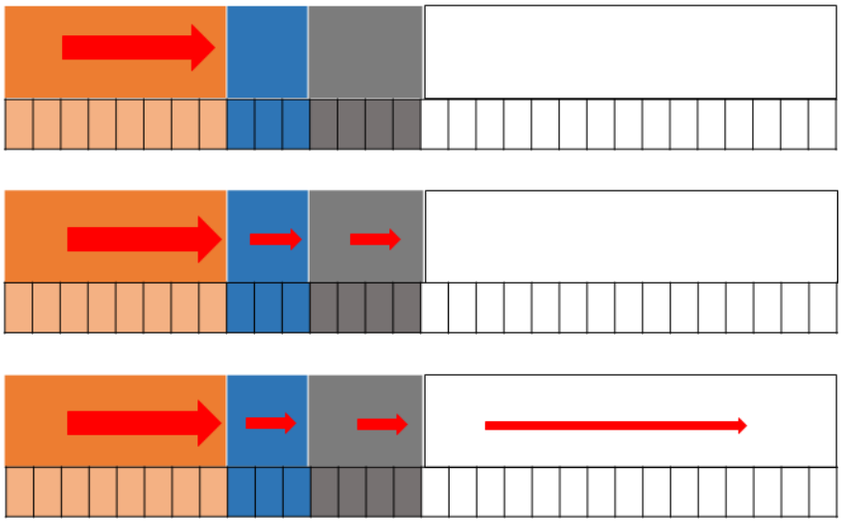

Figure 2.1: Model of the heat transfer through the finite elements of material

and the material properties of near elements for each item of the material itself. Through these data it calculates the heat exchange for each item and its nearest elements setting the upgraded temperature at the next temporal step. The simulation ends when a fixed portion of the cable reaches the critical density of current (function of the magnetic filed intensity and the temperature $J_{critic}(B,T)$ [4]) that corresponds to a value of temperature over the critical limit.

Chapter 3

Original Model: Simulation and Results

3.1 Simulation's Details

This model has the aim to verify if the consideration of the contact resistance could riproduce the measurement data taken at Fermilab. However, in the first place, I had to verify whether the model created could, in principle, have been approved. I decided to reproduce also the Simulation data made at Cern of the prototype tested at Fermilab to see if the model is reliable and could be used to predict the shape of the quench difference delay time considering the contact resistance. This model is very simple if compared to many programs of simulation like Roxie, Qlasa, Ansys, Comsol ecc. However, the purpose of my work is only to verify if the contact resistance has to be considered in the simulation of the heat transfer inside the superconducting magnets.

The main approximations of this model are:

- Heat generation: we supposed that in the stainless stell strips (heaters) the heat is firstly generated and then, when the simulation starts it flows through the insulation layers reaching the superconducting cable. We considered that the heaters absrorbed the heat reaching the temperature of 300 K, which is the intial value of temperature for all the material of the quench heaters. All the other material that we are considering in the simulation is made of insulation layers (which do not create heat) and superconducting material still under the critical surface, therefore, there are no other sources of heat. Thus, we can neglect the heat generation and study nothing but the heat propagation in the material.

- Constant material Properties: All the properties of the material we are considering in the simulation like the thermal conductivity, the specific heat or the material density are functions of the temperature. Because of this dependance, we need to recalculate, in the simulaiton, for each temporal step, all the material properties, considering the new value of the temperature for each finite element we created at the starting of the simulation. This continuos recalculation makes the real time for the run of the simulation very long. I supposed, for the first and original model, to consider all the material properties constants neglecting the temperature dependance. This approximation, despite being very strong because of the high order of dependance from the temperature of the material properties, was made only to create a very simplified and quick simulation of the quench delay time and quench difference delay time, in order to evaluate the consequence of the consideration of the contact resistance in the simulations. I took the value of all the material properties calculating them at the temperature of 1.9 K.

- Single finite element for the cable: considering the material properties we are using for the simulation, we evaluated that the ratio between the thermal conductivity of the cable and the thermal conductivity of the quench heaters is the following:

$$\frac{k_{cable}(T)}{k_{heater}(T)} \approx 100$$

we could then consider that the heat that reachs the surface of the cable that is in thermal contact with the insulation layers is quickly distributed in all the superconducting material. We thus considered that the superconducting cable could be concieved as like one finite element, simplifing so the heat exchange and the number of steps required to simulate the quench.

- Averaged value of magnetic field intensity. Considering for the superconducting cable only one finite element we can neglect the distribution of the magnetic field intensity in the superconducting material. The detection of the quench is simulated when the superconducting material reaches the temperature that correspond to a value of the current density over its critical limit. This critical point, however, is a function of the magnetic field intensity. In principle, each finite element has a different value of the critic current density. Considering only a unique finite element, we then have a unique determination of the quench inside the magnet. We do not consider the calculation of the minimum propagation zone for semplicity and also because of its difficult implementation in a finite element model. Consequently, we used a unique value of the magnetic field intensity for each simulated turn. We considered the average value of the magnetic field map taken with Roxie (figure: 1.2):

Turn HF (T)	**Turn LF (T)**
10	5.2

3.2 Results

We made simulations considering the contact resistance and neglecting this additional paramater in order to evaluate the difference in the quench delay time and in the quench delay time difference.

Here I reported the details of the simulations of the quench delay time for the HF turns and for the LF turns of the magnetic dipole.

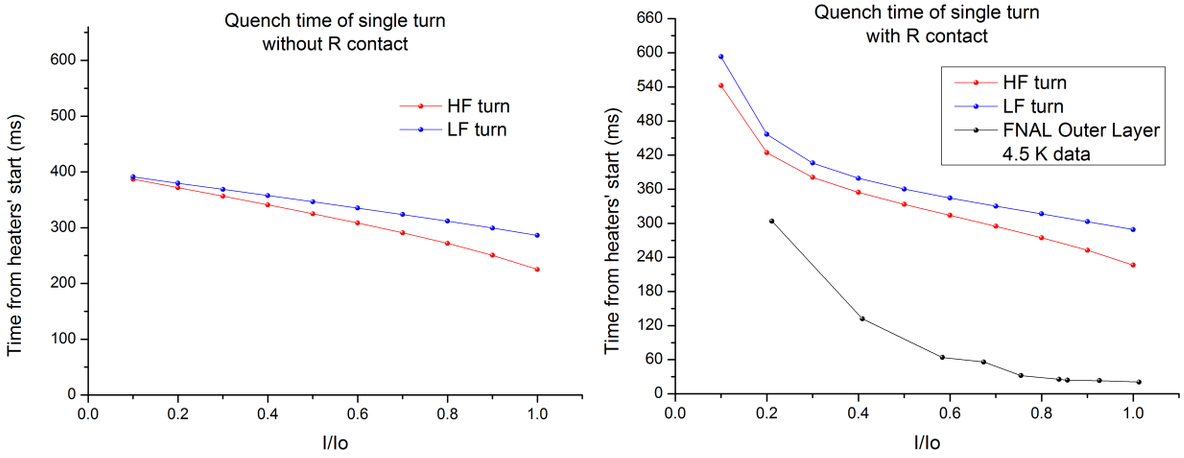

Figure 3.1: HF and LF turns single quench delay time considering or neglecting the contact resistance

Observations:

- As we expected from the observation on the operational points of the superconducting turns in the magnet, the single quench delay time of the HF turns is lower than the LF turns value. As I previously said, this behaviour is due to the different values of the magnetic field intensity at each value of current in the two turns of the magnet. Higher values of the magnetic field intensity can be considered in a lower value of the temperature margin or in a closer operational point of work to the critical surface.

- The shapes of the simulation data are very different if we consider the contact resistance or we neglect its contribute. Considering the contact resistance we obtain from the simulation a more similar shape of the data to the line's shape of the experimental data. However, the shape of the simulations and the data's one are still different even if we try to change the value of the coefficients in the parametrization of the contact resistance. We probably need to improve the dependance from the corrent, adding new coefficients in the parametrization, or the approximations, that we made to create this first model, are too tight and we need an upgrade of the model to have a better description of the quench delay time.

- Comparing the two plots of the simulations with the data from the measurements (in the second plot), we can see that, even if we consider or neglect the contact resistance, the values of the simulation results of the quench delay time are higher than the measurements values. There is an offset, that is a function of the current and so not costant for each point of the simulations, that we cannot delay adjusting the coefficients that we used in the parametrization of the contact resistance. In fact, considering the last values of the simulations

at high current, we can see that taking into account or neglecting the contact resistance, leads to the same result.

We also plotted together the simulations of the HF turns considering or neglecting the contact resistance and we made the same for the LF turns. As we observed in figures 3.1, we can see that

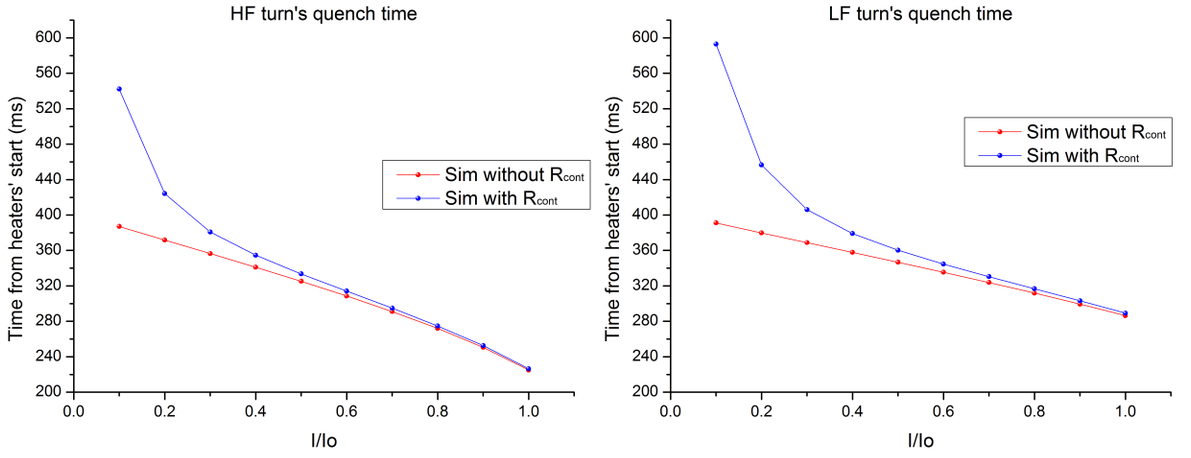

Figure 3.2: Compare for the HF turns and the LF turns of the simulaiton considering or neglecting the contact resistance

considering or neglecting the contact resistance for high values of the current leads to the same result in the quench delay time.

This behavior of the simulation can be observed also in the simulations of the quench delay time difference that we report here:

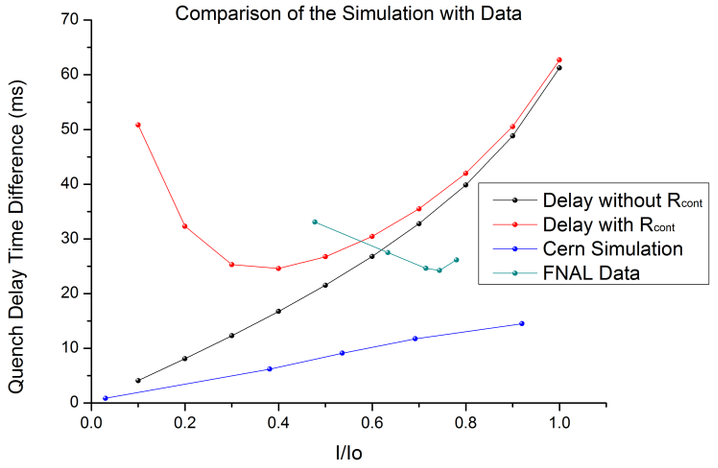

Figure 3.3: Simulation of the quench delay time difference considering or neglecting the contact resistance and compare with previous simulation and experimental data

From the analysis of this simulation we can observe: The positive elements can be summarized in two observations.

- Considering the contact resistance at low operational current, the quench delay time difference increases as the measurements do when the current goes to the zero value. This particular behaviour is one of the main goal we are trying to reach with our simulations but, in principle, we do not expect that the quench delay time difference goes to infinite as the current goes to zero. As the current goes to zero, the difference of the magnetic field intensity goes to zero too because the magnetic field is proportional to the current itself. If the difference in the magnetic field is null, and so null is also the difference in the operational point for the two considered turns, the single quench delay time has to be the same because the contribution of the different contact resistance becomes negligible compared to this same physical condition. We therefore expect a maximum in the quench delay time difference shape at a low value of current but a null value of this parameter for null values of the x-axis.

- At high current, the simulation considering the contact resistance, as we previously observed for the single quench delay time, converges to the same value of the simulation that neglect the additional parameter. From this behaviour we can recognize that the value of the contact resistance, for this range of current, becomes negligible compared to the thermal resistance of the material. Because of we do not observe the same behaviour of the quench delay time difference in the experimental data and in the Cern simulation, we have to select values of the coefficients in the parametrization that make the contact resistance not negligible if compared to the thermal resistance of the material.

Instead, bad elements of the simulation are the following:

- The simulation without considering the contact resistance cannot reproduce the Cern simulation making for us not possible to rely on this appoximated model for the determination of the contact resistance itself. Firstly, we have to reproduce the Cern simulation that does not take into account the contact resistance, in order to validate our model. Only if we validate our model, we can predict and calculate the contact resistance for the interface between the G10 and the superconducting cable.

- At high value of current the quneh delay time difference, taking into account or negliecting the contact resistance, seems to diverge before saturating. This behaviour, in principle, is not expected because at high current the single quench delay time of the turns is expected to goes to a very low but finite value. The divergence is not physically acceptable and so this behaviour is probably due to a problem of our model.

Chapter 4

Upgraded Model: Simulation and Results

4.1 Simulation's and upgrade's details

From the results of the first model we have obtained that the contact resistance could be a possible solution to the problem of the discrepancy in the quench delay time difference determination between the simulations and the experimantal data.

However, to calculate the exact value of this additional parameter through the simulation, we have to reproduce the Cern simulation that does not take into account the contact resistance. We have observed, in the first model, that the approximations that we made for it were too strong. We need more precision in the determination of the material properties, at first, and we have to verify if the implementation of the in-time generation of the heat has a non negligible effect on the calculation of the single quench delay time and, therefore, also in the quench delay time difference.

To exactly reproduce the Cern simulation, we used in this upgraded model the parametrization of all the material properties as functions of the temperature of the material itself. For this parametrizations we used the value of the material properties at cryogenic temperatures from the NIST database which all the simulations made by Cern rely on [5]. The Nb_3Sn Heat Conductivity and Specific Heat are taken from MATPRO parametrization because of the difficult description of this parameters from the Magnetic Field Intensity in which the material works at cryogenic temperatures.

We plotted the material properties in the range of temperature between 0 and 300 K to analyze if the parametrization we used has no discontinuity and can be reliable for all the temperature that the finite elements in the simulation reach during the run.

We studied the material properties of the copper because we considered also in this upgraded model the complicated composition of the cable. We did not consider the spatial distribution of the different material that compose the cable but we considered a weighted average on their proportions to determine the values of the specific heat, the heat conductivity and the density for the finite elements of the cable [6].

The proportions of the different materials in the cable are:

$$Cu(35.25\%), \quad Nb_3Sn(39.85\%), \quad EpoxyFiberglass(24.9\%)$$

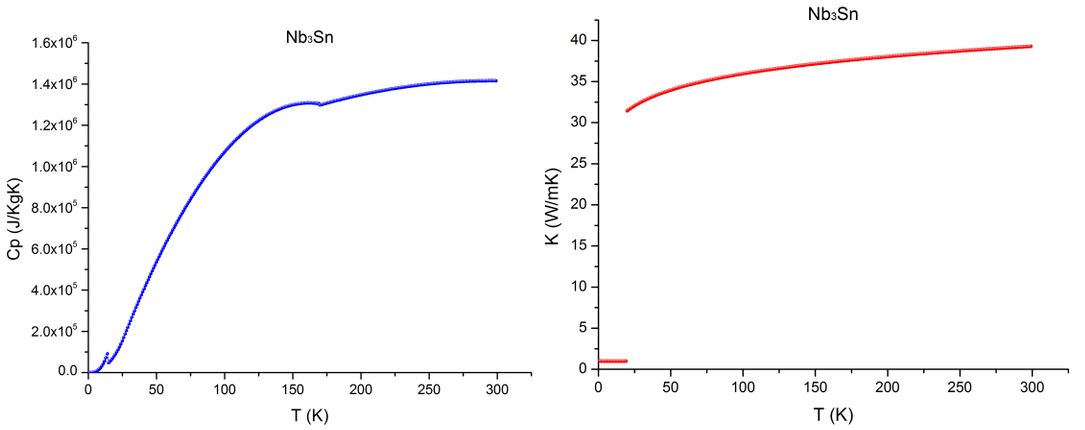

Figure 4.1: Nb_3Sn Specific Heat ($\frac{J}{KgK}$) and Heat Conductivity ($\frac{W}{mK}$)

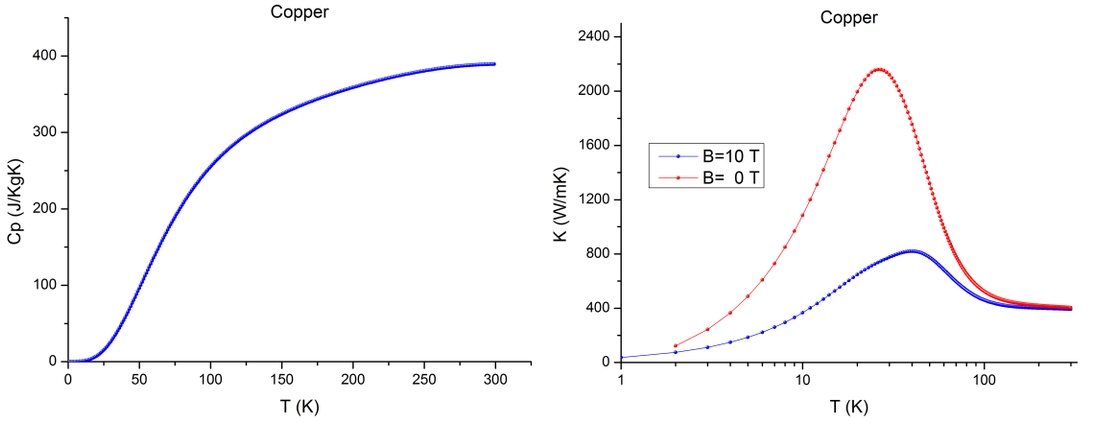

Figure 4.2: *Copper* Specific Heat ($\frac{J}{KgK}$) and Heat Conductivity ($\frac{W}{mK}$)

We can observe the complicated dependence of the Heat Conductivity of the Nb_3Sn on the temperature and the dependance of the Specific Heat of the Copper on the Magnetic Field strength in which the material works. We can see from the plot of the Heat Conductivity of the Nb_3Sn that we have a critic discontinuity of this parameter. This is due only on the parametrization that we have used for the description of this material properties because, in the reality, this discontinuity is absent in the measurements and tests on short sample of the material. We have so to consider the impact of this bad description on our results of the model and we have to use a different parametrization that creates a continuos shape in the range of the cryogenics temperatures that we are using for the simulations. We have so, compared to the First Model in which we used constant value of the material properties, a more complicated and useful description of all the crucial parameters that are important for the resolution of the heat transfer equation.

We implemented in the program, for each temporal step, the recalculation of the material properties as function of the temperature, to see the dependance of our result from the parametrization that we are using. Because we calculated the material properties as functions of the temperature, it is necessary to divide the cable in finite elements, thus making the simulation closer to the real

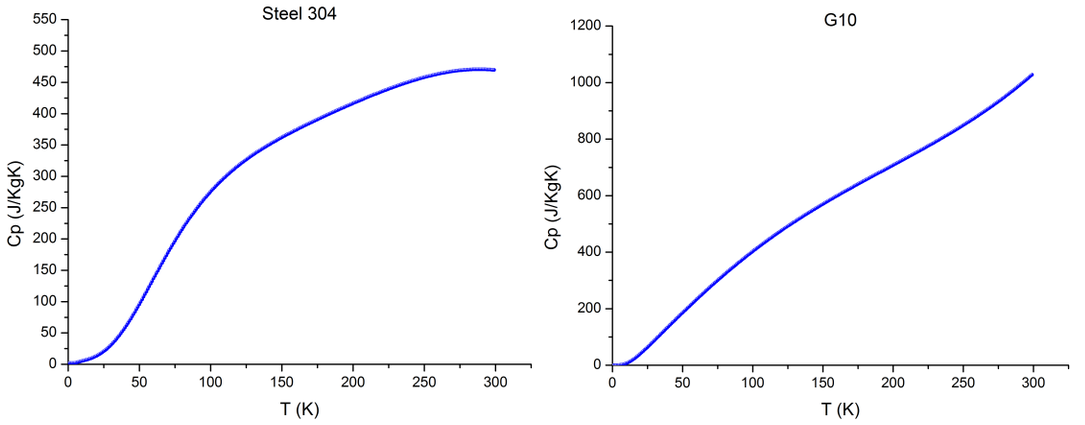

Figure 4.3: Specific Heat for Stainless Steel 304 and G10 ($\frac{J}{KgK}$)

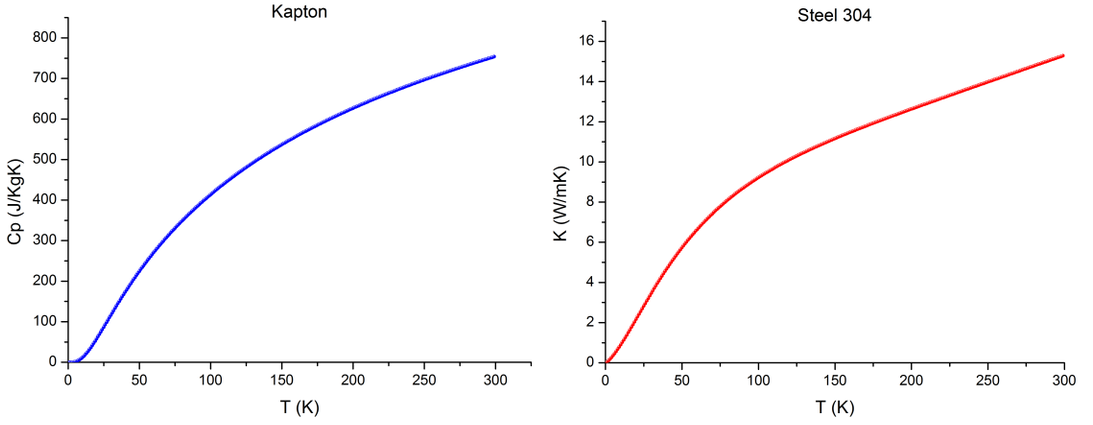

Figure 4.4: Specific Heat ($\frac{J}{KgK}$) of Kapton and Heat Conductivity ($\frac{W}{mK}$) of the Stainless Steel 304

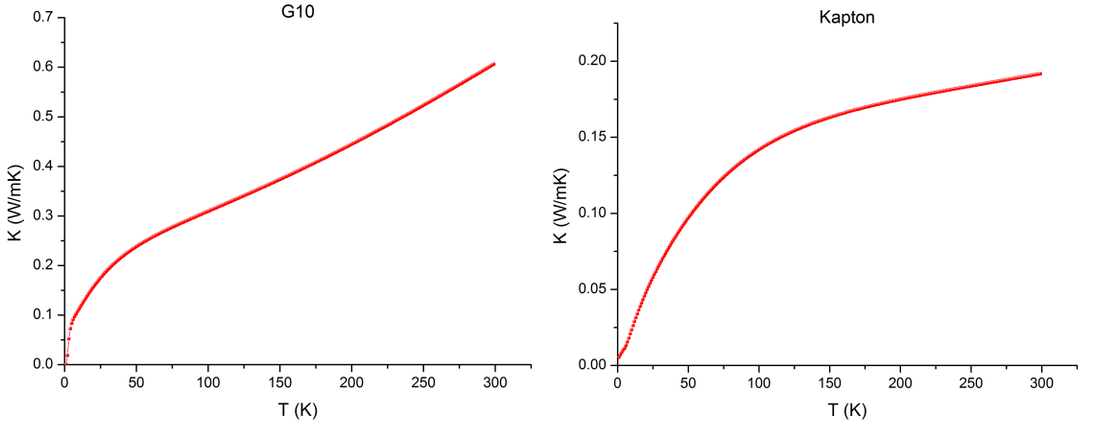

Figure 4.5: Heat Conductivity for G10 and Kapton ($\frac{W}{mK}$)

process.

However, in the first model, we could use the average of the magnetic field because we had only one finite element for the total turn. For this upgraded model we decided to considered the maximum value of the magnetic field and not the avarage value to get closer to the real critical point of the cable having more precision in the determination of the single quench delay time.

Turn HF (T)	**Turn LF (T)**
10.5	5.8

4.2 Results

Here we report the results that we obtained from simulations that use the bew material properties and in which we selected for the parameters of the contact resistance the following values:

$$\alpha = 2 \cdot 10^{-5} \qquad \beta = 0.4$$

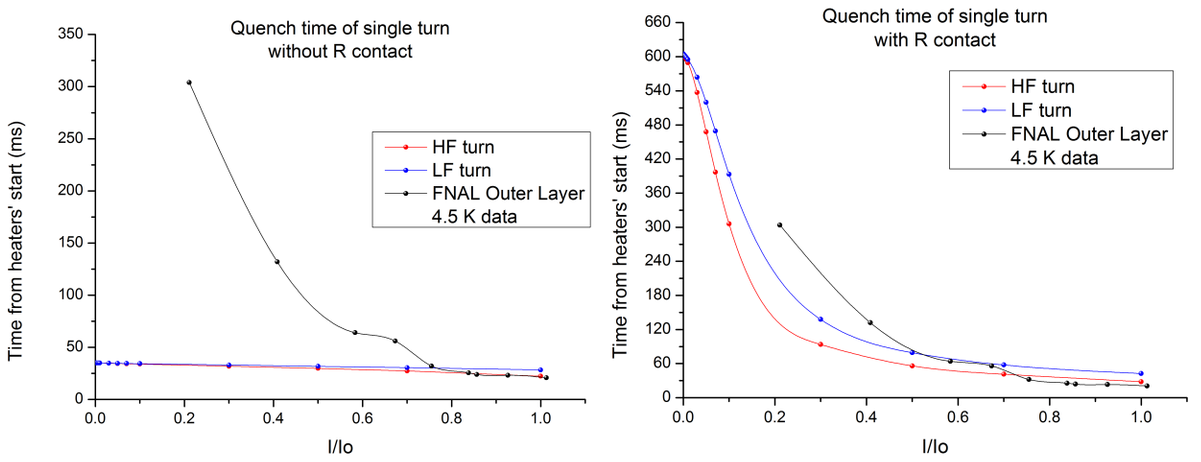

Figure 4.6: Single quench delay time for HF Turns and LF Turns taking into account or neglecting the contact resistance

We can observe, from the plots 4.6, that the offset we saw in the First Model, between our simulations and the FNAL Data, has completely disappeared and for high value of the current our simulation are compatible with the FNAL data. Without considering the contact resistance, the single delay times cannot describe the shape of the FNAL Data. In fact, all the values of the simulations lie below the value of 34 ms while the FNAL data reach values over 300 ms for small values of the current. Instead, taking into account the contact resistance we can see that we are able to reproduce the decay of the quench dealy time as funciton of the current even if there is a different rate of the decay between our simulation and the experimantal data. We tried to change the parameters of the contact resistance to reproduce the decay but we decided to maximize the agreement of the quench delay time difference with the experimental data of this last parameter. Probably, adding new coefficients in the parametrization of the contact resistance, improving the

order of the polynomial dependance from the Pressure, we should be able to reproduce both the single quench delay time and the quench delay time difference.

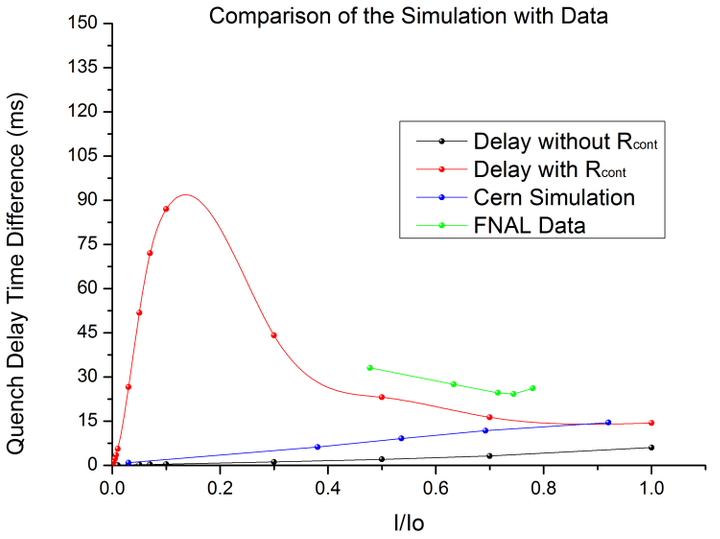

Figure 4.7: Simulation of the quench delay time difference considering or neglecting the contact resistance.

For this new upgrade of the model we extended the analysis of the quench dealy time and the quench delay time difference also to low value of the current to see the behaviour of these parameters.

As we expected (see figure 4.7), the quench delay time difference at low values of current goes to 0, the operational points of work being closer and closer and becoming dominant on the non negligible values of the contact resistances for the HF and LF turns. It is therefore created a maximum value of the quench delay time difference that is a function of the values of the parameters we selected for the contact resistance. We can see that, for the values of the parameters we used for this simulations, we can describe very well the shape of the quech difference delay time in the same range of current in which there are the experimantal data. However, the simulation and the experimental data do not overlap and there seems to be an offset between them that we cannot delete changing the parameters of the contact resistance. Another problem affects the simulation without considering the contact resistance. If in the previous model we overexstimated the value of the quenh difference dealy time, in this model, we underexstimate this parameter. We supposed a problem in the heat generation. In fact, if we overexstimate the value of the heat created in the material (we selected 300 K of beginning temperature for the quench heaters), we expect an understimate value of the single quench delay time and the quench delay time difference. Then, we decided to modify the generation of the heat considering a in-time production while the heat flows through the insulation layers. We simulated the real decay of the power generated in the heaters. The behaviour of the generated Power density from the time can be described by an exponential decay because the energy given to the heaters is firstly accumulated in a Electrical Capacity that is discharged when the detection of the quench in the cable is activated. We used the Minimum Power Density to induce the quench in the cable using the parameters describe in tabular 4.2.

The decay time τ is measured experimentally from the electrical capacity that is discharged on

Peak Power Density W/cm^2	Tau ms	Test
25.23	37.152	MBHSP01
55.82	31.296	MBHSP02

the quench heaters and the electrical resistivity of the quench heaters itself. We need to modify the equation of the heat transfer considering the generation of heat in the quench heaters: returning to the first equation

$$\frac{\partial}{\partial x}\left[k(T)\frac{\partial T}{\partial x}\right] + \frac{\rho(T)I^2}{A^2} = c_p^c(T)\delta(T)\frac{\partial T}{\partial t}$$

we can rewrite the electrical resistivity to the peak power density and its value as function of time. Simplifing the equation making all thye parameters adimensional we can obtaine:

$$\theta_{i,j+1} = \theta_{i,j} + \frac{r}{(\tilde{c}_p^c)_{i,j}\tilde{\delta}_{i,j}}\left[\tilde{k}_{i,j}(\theta_{i,j+1} - 2\theta_{i,j} + \theta_{i-1,j}) + \frac{1}{4}\left(\frac{\partial\tilde{k}}{\partial\theta}\right)_{i,j}(\theta_{i+1,j} - \theta_{i-1,j})^2\right] + \frac{\delta Q_i}{(\tilde{c}_p^c)_{i,j}}$$

where the last part of the equation is the additional term that takes into account the generation of the heat.

$$\frac{\delta Q_i}{(\tilde{c}_p^c)_{i,j}} = \frac{Power_{i,j}}{\Delta l}\frac{kL^2}{k_0(T_0)T_0(\tilde{c}_p^c)_{i,j}\delta_{i,j}}$$

We can observe that the additional parameters is a function of the initial parameters that we selected in the simulation but this dependance is due only to the simplification that we made to rewrite the equation. Physically this additional term is only a function of the instantanous power density and the thickness of the quench heater.

Here in figure 4.8 we report the simulations made with the new configuration of the heat generation and the new parametrizations of the coefficients for the material properties.

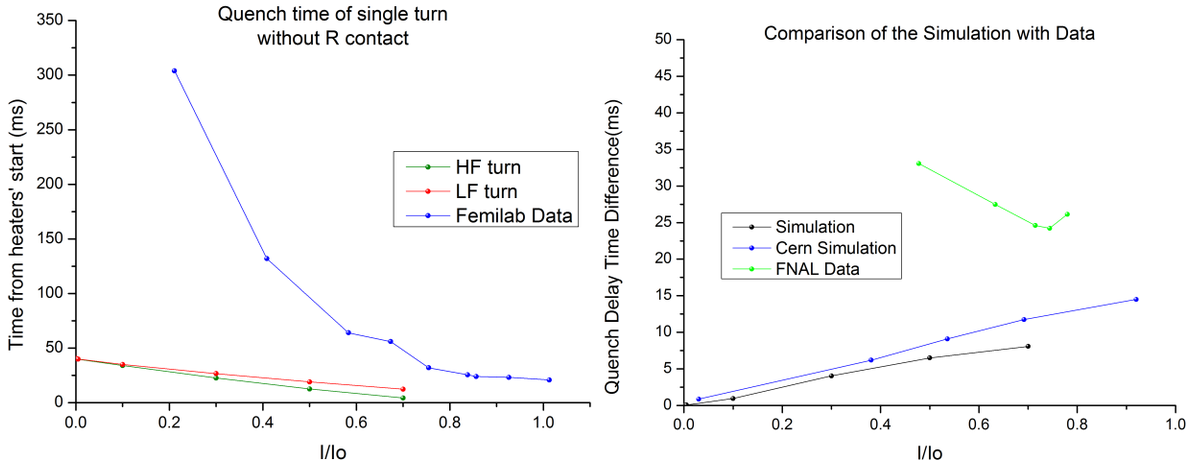

Figure 4.8: Single quench delay time and quench delay time difference without taking into account the contact resistance.

In these plots we can see the comparison between the experimental data, the Cern's simulaiton and our simulation without taking into account the contact resistance. The execution of simulations that consider the contact resistance take too much time without a grid of computer or a parallelized code that could simplify the computing in the program. Therefore, in the end, we have only the results of the simulation that does not consider the contact resistance.

We can observe from the plots that without taking into account the contact resistance we cannot describe the decay of the quench delay time with higher values of the current. A positive element of this simulation is the reproduced behaviour of the quench delay time difference. For low value of the current our simulation and Cern's one are compatible, while for higher values of the corrent there is more quickly saturation. Probably, this different behaviour is due to the different way through which we determine the quench in the cable. Our simulation uses a fixed dimensional size that has to reach the critical surface of the superconductor material to determine the quench in the cable, while the Cern simulation uses a more complicate calculation of the minimum propagating zone that is a function of the material exchange of heat and the heat generation of the superconducting material, that in our simulation is not taken into account for simplicity.

Conclusions

The aim of my work was the introduction of a new Contact Resistance in the study of the heat transfer from the quench heaters and the superconducting cable as possible solution for the discrepancy between simulation and experimental results in the calculation of the quench delay time difference. My work focuses on the development of a C++ code to recreate through simulatios the heat transfer calculating and parametrizing also the main dependance of the Contact Resistance on the operational current in the superconducting magnet. We saw, from the first model, that the introduction of this new parameter create an increase of the quench delay time difference as the current is lower and lower as the measurements, taken in experimental tests of the 11 T dipole Magnet prototype both at Cern and Fermilab, show. We upgraded the first model, removing many of the approximation we made to create a very simple program, and we firstly obtained:

- Introducing the contact resistance in the heat transfer it is possible, depending on the parametrization of the additional resistance, to reproduce the similar shape of the measurements in their range of current, in which they were taken, while, in lower range of the operational current, predict the behaviour of the quench delay time difference, in particular in values of current close to 0.
- We showed that the contact resistance has to be considered to well describe the behaviour of the quench delay time and quench delay time difference reproducing the Cern Simulation with our model that does not take into account this additional parameter in the heat transfer.
- We used the cern simulation to make our program and our model reliable to predict the correct parametrization of the contact resistance as funciton of the current in the magnet.

Unfortunately, we could not select the best value of the coefficients in the parametrization of the contact resistance for the most complicate model we created because of the long time that the simulations take to calculate the singles quench delay time and their differences. We just started simulations of the new model considering the contact resistance after improvement in the c++ code to make it more quick in the calculations. After having determined the best coefficients for the contact resistance parametrization, we have to improve our model in the calculation of the precise time in which the quench is detected. To determine this value of time we need to implement the calculation of the minimum propagating zone in the superconducting cable considering also the heat generated by the finite elements that reach the normal conductive state. We could also consider to use of other programs that are more complicate than ours, improving their model with the value of the contact resistance that we will obtaine from our simulations.

Bibliography

[1] A. Zlobin, N. Andreev, G. Apollinari, B. Auchmann, E. Barzi, S. I. Bermudez, R. Bossert, M. Buehler, G. Chlachidze, J. DiMarco, M. Karppinen, F. Nobrega, I. Novitski, L. Rossi, D. Smekens, M. Tartaglia, D. Turrioni, and G. Velev, "11 T Twin-Aperture Nb_3Sn Dipole Development for LHC Upgrades," *IEEE Transactions on Applied Superconductivity*, vol. 25, June 2015.

[2] E. Barzi, "Gas/Vapour-cooled binary current leads - Copper part," *FNAL Technical division Report*, vol. TD-98-026, Mar 1998.

[3] T. Salmi, D. Arbelaez, S. Caspi, H. Felice, S. Prestemon, LBNL, Berkeley, CA, 94720, USA, G. Chlachidze, F. N. Laboratory, IL, USA, H. H. J. ten Kate, and U. of Twente Enschede Netherlands, "Modeling heat transfer from quench protection heaters to superconducting cables in Nb_3Sn magnets," *CERN Yellow Report*, vol. CERN-2013-006, June 2015.

[4] L. T. Summers, M. W. Guinan, J. R. Miller, and P. A. Hahn, "A model for the prediction of Nb_3Sn critical current as a function of field, temperature, strain, and radiation damage," *IEEE Transactions on Applied Superconductivity*, vol. 27, Mar 1991.

[5] G. Manfreda, "Review of ROXIE's Material Properties Database for Quench Simulation," *CERN Technology Department*, vol. Internal Note 2011-24, Dec 2011.

[6] T. Salmi, D. Arbelaez, S. Caspi, H. Felice, M. G. T. Mentink, S. Prestemon, A. Stenvall, and H. H. J. ten Kate, "A Novel Computer Code for Modeling Quench Protection Heaters in High-Field Nb_3Sn Accelerator Magnets," *IEEE Transactions on Applied Superconductivity*, vol. 24, Aug 2014.